of DNFB-sensitized LN cells in a ratio as low as 1:100 (Tregs to LN cells), but such an inhibitory effect was not observed in non-antigen-specific mitogen-induced T cell proliferation systems. Therefore, Tregs circulating between the skin and LNs may inhibit not only T cells, but also antigen-presenting cells, such as dendritic cells, or antigen-presenting cell-T cell interactions. Moreover, subcutaneous injection of migratory Tregs into the skin suppressed CHS more markedly than that of LN-resident Tregs. Similar findings were observed when these Tregs were transferred intravenously (data not shown), suggesting that Tregs migrating from the skin hold a high immunosuppressive potential.

The $CD25^{high}$ subset that migrated from the skin seems to have an activated phenotype, indicated by the positivity of CD25 and CD103. It has been reported that transfer of pre-activated $CD25^{+}CD103^{+}$ cells strongly suppressed T cell proliferation (32) and $CD25^{+}CD103^{+}$ cells are the main producer of IL-10 after TCR stimulation (29). The $CD25^{high}$ subset in our finding express high levels of CD103 and IL-10, and strong suppressive capacity and phenotype, consistent with an activated effector/memory Treg subset (28, 33). It should be noted that we demonstrate that $CD25^{high}$ subset was localized in the skin and only transiently migrated from the skin after CHS-elicitation. Thus, the role of skin in generation, education and spatiotemporal regulation of this $CD25^{high}$ subset during immune responses needs to be elucidated in the future, which may lead us to understand the role of peripheral tissues in regulation of immune responses.

Notably, Treg cell circulation was remarkably induced during cutaneous immune responses. Therefore, we have focused on the roles of Tregs instead of effector/memory T cells migrating from the skin. In fact the administration of migratory Tregs strongly suppressed CHS response at the later phase after a challenge (Figure 5A) and that *in vivo* depletion of Tregs prolonged the CHS response particularly during the later phase (Figure 4B). These results suggest that these

circulating Tregs might be involved in the termination of immune responses. However, immune responses and homeostasis are regulated and maintained by the balance between Tregs and effector/memory T cells, and it has been thought that CHS occurs by the dominance of effector/memory T cells over Tregs. Hence, it is intriguing that the elicitation of CHS induces Tregs despite their possible antagonistic role for the development of acquired immune response. In this sense, it will be of interest to explore more the roles of effector/memory T cells and Tregs migrating from the skin in regulating immune response. Clarification of these issues will lead not only to understanding of the novel mechanism of cutaneous immune responses, but also to control of systemic immune responses through modulating cutaneous immunity.

Methods

Mice and photoconversion

Tg mice carrying Kaede cDNA under the CAG promoter were established previously(17). These mice with C57BL/6 (B6) genetic background expressed photoconvertible Kaede in all of their cell types. It should be noted that the use of violet light (436 nm) rather than harmful UVA (320–400 nm) or UVB (290–320 nm) allowed us to photoconvert Kaede in the cells with no detectable damage (17).

Because of the moiety of its wavelength, violet light exposure penetrates through the skin to subcutaneous tissue, but not further (data not shown). Although the exposure of Kaede to violet light permanently changes its structure, and photoconverted Kaede has a very long biological half-life in lymphocytes, cell proliferation dilutes photoconverted Kaede with newly synthesized non-photoconverted Kaede, and after several cell divisions the detection of red fluorescence becomes difficult (17). Moreover, exposure of the cells to violet light for 10 min has no effect on T and B cell proliferation (17). To exclude the immunomodulatory effect of photoconversion *in*

vivo, we used the contact hypersensitivity (CHS) model. Photoconversion of the abdominal skin immediately after sensitization on the abdomen did not affect CHS response (data not shown). When mRNA level of *Il1β* was examined 6 h after photoconversion (436 nm) or low-dose (3 kJ/m^2) UVB exposure, significant increase of mRNA level of *Il1β* was observed by UVB but not by photoconversion (Supplemental Figure S8). Therefore, we assume that photoconversion of the skin does not provoke significant inflammation in the skin or inflammatory stimuli in keratinocytes.

B6 Foxp3$^{hCD2/hCD52}$ mice were generated by homologous recombination in a B6-derived ES cell line using a targeting construct in which cDNA encoding a human CD2 and human CD52 fusion protein along with an intra-ribosomal entry site was inserted into the 3' un-translated region of the endogenous Foxp3 locus (18). All CD4$^+$ Foxp3$^+$ cells expressed hCD2, but CD4$^+$ Foxp3$^-$ cells did not (data not shown) indicating that the expression of the human CD2 reporter faithfully reflects the intracellular expression of Foxp3 in Foxp3$^{hCD2/hCD52}$ mice. Foxp3$^{hCD2/hCD52}$ mice (18) were intercrossed with Kaede-Tg mice to generate Kaede/Foxp3$^{hCD2/hCD52}$ mice for further evaluation. These mice were bread in specific pathogen-free facilities at Kyoto University or RIKEN. All experimental procedures were approved by the Institutional Animal Care and Use Committee of Kyoto University Faculty of Medicine and RIKEN.

Antibodies and flow cytometry

Fluorochrome-conjugated or biotinylated anti-human CD2, anti-mouse CD4, CD11a, CD11c, CD25, CD44, CD45RB, CD62L, CD69, CD103, glucocorticoid-induced TNFR family-related gene/protein (GITR), CCR4, CCR5, and CCR7 mAbs were obtained from BD Biosciences (San Diego, CA), eBioscience (San Diego, CA), or

Biolegend (San Diego, CA). Data were acquired using the JSAN system (Baybioscience, Kobe, Japan) or FACSCanto II flow cytometry system (BD Biosciences) and analyzed with FlowJo (TreeStar, San Carlos, CA).

Cell preparation from the skin and cell sorting

Briefly, the ears were removed and split into dorsal and ventral halves, and cartilage was removed. The skin of the ears was floated on 0.25% trypsin/EDTA for 30 min at 37°C. Then, the epidermis was peeled from the dermis, and both epidermis and dermis were minced with forceps. The minced tissues were incubated for 1 h in collagenase II (Worthington, Biochemical, Freehold, NJ) containing hyaluronidase and DNaseI (Sigma). The cell suspensions were filtered with 40 μm of cell strainer.

For cell sorting, Kaede-red Tregs or Kaede-green Tregs were purified from inguinal and axillary LNs of Kaede/Foxp3$^{hCD2/hCD52}$ mice. Briefly, the mice were sensitized and challenged with 2,4-dinitro-1-fluorobenzene (DNFB) in the same way as the B6 mice for 2,4-dinitrobenzene sulfonic acid (DNBS)-induced cell proliferation. Two days after the challenge, cells of abdominal skin were photoconverted, and single cell suspensions were prepared from inguinal and axillary LNs 24 h after photoconversion. The cells of each population were sorted by the FACSAria II flow cytometry system (BD Bioscience).

Photoconversion, CHS model, *in vivo* Treg depletion, and cell proliferation assay

Photoconversion of the skin was performed as described previously (17). Briefly, mice were anesthetized, shaved and exposed to violet light at 95 mW/cm^2 with a 436-nm bandpass filter using Spot UV curing equipment (SP500; Ushio, Tokyo, Japan).

For the CHS model, mice were immunized by application of 25 μl of 0.5% DNFB (Nacalai Tesque, Kyoto, Japan) in 4:1 (wt/vol) acetone/olive oil to their shaved abdomens on day 0 and challenged on the right ear on day 5 with 20 μl of 0.3%

(wt/vol) DNFB (34). Ear thickness was measured before and after challenge, and ear thickness change was calculated.

For Treg depletion *in vivo*, mice were injected with Campath-1G Ab through the tail vein (0.5mg/body) one day before the CHS challenge (22). The injection was repeated every four days throughout the experiment. The same amount of vehicle or rat IgG (0.5mg/body; Sigma, St. Louis, MO) was used as a control.

For DNBS- or trinitrobenzene sulfonic acid (TNBS)-dependent cell proliferation, mice were sensitized with 50 μl of 0.5% DNFB (wt/vol) or 50 μ l of 5% 2,4,6-trinitro-l-chlorobenzene (TNCB) (Tokyo Kasei) (wt/vol) in acetone/olive oil (4/1; vol/vol) on the dorsal skin, and 5 days later, single-cell suspensions were prepared from inguinal and axillary LNs. CD25-positive cells were depleted from the cells by Auto-MACS (Miltenyi Biotec, Bergisch Gladbach, Germany) using PE-labeled anti-mouse CD25 antibody (eBioscience) and magnetic microbeads coated with anti-PE (Miltenyi Biotec). Less than 1% of $Foxp3^+$ cells were present in the remaining LN cells. 7 x 10^5 LN cells/well in a 96-well plate were cultured in RPMI 1640 containing 10% FBS with or without 50 μg/ml DNBS (Alfa Aesar, Ward Hill, MA) for 3 days. For TNBS-stimulation, the LN cells were incubated in 2.5mM TNBS (Tokyo Kasei, Tokyo, Japan) in PBS for 20 min at 37°C, subsequently washed 3 times in PBS, and 7 x 10^5 cells/well in a 96-well plate were cultured in RPMI 1640 containing 10% FBS for 3 days. Cells were pulsed with 0.5 μCi ^{3}H-thymidine for the last 24 h of culture and subjected to liquid scintillation counting.

For the proliferation assay of anti-CD3 stimulation, spleen $CD4^+$ cells deprived of $CD25^+$ cells were sorted by auto-MACS. Then, 5 x 10^4 cells/well were cultured in a 96-well plate coated with 1 μg/ml of anti-CD3 antibody for 72 h. For the last 24 h, cells were pulsed with 0.5 μCi ^{3}H-thymidine and its incorporation was measured.

Quantitative RT-PCR analysis

Total RNA from purified cells was isolated with the RNeasy mini kit (QIAGEN, Venlo,

Netherlands). Quantitative RT-PCR with the Light Cycler real-time PCR apparatus was performed according to the instructions of the manufacturer (Roche) by monitoring the synthesis of double-stranded DNA during the various PCR cycles using SYBR Green I (Roche, Basel, Switzerland). For each sample, duplicate test reactions were analyzed for expression of the gene of interest, and results were normalized to those of the *Gapdh* mRNA.

In vivo immunosuppression assay

A total of 4 x 10^3 cells of isolated Kaede-red Tregs or Kaede-green Tregs in 20 μl PBS were subcutaneously injected into the ventral surface of each ear. Ear thickness was measured for each mouse before and at the indicated time point after elicitation with a micrometer, and the difference was expressed as ear swelling (N=4~6 in each group).

Chemotaxis assay

Skin cell suspensions of Foxp3$^{hCD2/hCD52}$ mice were tested for transmigration across uncoated 5-μm transwell filters (Corning Costar Corp., Corning, NY) for 3 h to CCL21 (R&D systems, Minneapolis, MN) or medium in the lower chamber, and the numbers of cells that migrated to the lower chamber were determined by flow cytometry (35). The migration index was shown as a percentage of input by dividing with total input cells in upper chamber.

Statistical analysis

Data were analyzed with the unpaired two-tailed *t*-test unless otherwise stated. A *P* value of less than 0.05 was considered to be significant.

ACKNOWLEDGEMENTS

This study was supported in part by grants from the Ministry of Education, Culture, Sports, Science, and Technology of Japan, and the Ministry of Health, Labor, and Welfare of Japan.

REFERENCES

1. Korn, T., Bettelli, E., Oukka, M., and Kuchroo, V.K. 2009. IL-17 and Th17 Cells. *Annu Rev Immunol* 27:485-517.
2. Sakaguchi, S., Yamaguchi, T., Nomura, T., and Ono, M. 2008. Regulatory T cells and immune tolerance. *Cell* 133:775-787.
3. Lu, L.F., and Rudensky, A. 2009. Molecular orchestration of differentiation and function of regulatory T cells. *Genes Dev* 23:1270-1282.
4. Gowans, J.L., and Knight, E.J. 1964. The Route of Re-Circulation of Lymphocytes in the Rat. *Proc R Soc Lond B Biol Sci* 159:257-282.
5. Gowans, J.L. 1959. The recirculation of lymphocytes from blood to lymph in the rat. *J Physiol* 146:54-69.
6. Mackay, C.R., Marston, W.L., and Dudler, L. 1990. Naive and memory T cells show distinct pathways of lymphocyte recirculation. *J Exp Med* 171:801-817.
7. Matloubian, M., Lo, C.G., Cinamon, G., Lesneski, M.J., Xu, Y., Brinkmann, V., Allende, M.L., Proia, R.L., and Cyster, J.G. 2004. Lymphocyte egress from thymus and peripheral lymphoid organs is dependent on S1P receptor 1. *Nature* 427:355-360.
8. Campbell, D.J., Debes, G.F., Johnston, B., Wilson, E., and Butcher, E.C. 2003. Targeting T cell responses by selective chemokine receptor expression. *Semin Immunol* 15:277-286.
9. Campbell, J.J., Haraldsen, G., Pan, J., Rottman, J., Qin, S., Ponath, P., Andrew, D.P., Warnke, R., Ruffing, N., Kassam, N., et al. 1999. The chemokine receptor CCR4 in vascular recognition by cutaneous but not intestinal memory T cells. *Nature* 400:776-780.
10. Homey, B., Alenius, H., Muller, A., Soto, H., Bowman, E.P., Yuan, W., McEvoy, L., Lauerma, A.I., Assmann, T., Bunemann, E., et al. 2002. CCL27-CCR10 interactions regulate T cell-mediated skin inflammation. *Nat Med* 8:157-165.
11. Olszewski, W.L., Grzelak, I., Ziolkowska, A., and Engeset, A. 1995. Immune cell traffic from blood through the normal human skin to lymphatics. *Clin Dermatol* 13:473-483.
12. Olszewski, W.L. 2003. The lymphatic system in body homeostasis: physiological conditions. *Lymphat Res Biol* 1:11-21; discussion 21-14.
13. Mackay, C.R., Kimpton, W.G., Brandon, M.R., and Cahill, R.N. 1988. Lymphocyte subsets show marked differences in their distribution between blood and the afferent and efferent lymph of peripheral lymph nodes. *J Exp Med* 167:1755-1765.

14. Debes, G.F., Arnold, C.N., Young, A.J., Krautwald, S., Lipp, M., Hay, J.B., and Butcher, E.C. 2005. Chemokine receptor CCR7 required for T lymphocyte exit from peripheral tissues. *Nat Immunol* 6:889-894.
15. Ando, R., Hama, H., Yamamoto-Hino, M., Mizuno, H., and Miyawaki, A. 2002. An optical marker based on the UV-induced green-to-red photoconversion of a fluorescent protein. *Proc Natl Acad Sci U S A* 99:12651-12656.
16. Mizuno, H., Mal, T.K., Tong, K.I., Ando, R., Furuta, T., Ikura, M., and Miyawaki, A. 2003. Photo-induced peptide cleavage in the green-to-red conversion of a fluorescent protein. *Mol Cell* 12:1051-1058.
17. Tomura, M., Yoshida, N., Tanaka, J., Karasawa, S., Miwa, Y., Miyawaki, A., and Kanagawa, O. 2008. Monitoring cellular movement in vivo with photoconvertible fluorescence protein "Kaede" transgenic mice. *Proc Natl Acad Sci U S A* 105:10871-10876.
18. Komatsu, N., Mariotti-Ferrandiz, M.E., Wang, Y., Malissen, B., Waldmann, H., and Hori, S. 2009. Heterogeneity of natural Foxp3+ T cells: a committed regulatory T-cell lineage and an uncommitted minor population retaining plasticity. *Proc Natl Acad Sci U S A* 106:1903-1908.
19. Fontenot, J.D., Rasmussen, J.P., Gavin, M.A., and Rudensky, A.Y. 2005. A function for interleukin 2 in Foxp3-expressing regulatory T cells. *Nat Immunol* 6:1142-1151.
20. Randolph, G.J., Ochando, J., and Partida-Sanchez, S. 2008. Migration of dendritic cell subsets and their precursors. *Annu Rev Immunol* 26:293-316.
21. Hirahara, K., Liu, L., Clark, R.A., Yamanaka, K., Fuhlbrigge, R.C., and Kupper, T.S. 2006. The majority of human peripheral blood CD4+CD25highFoxp3+ regulatory T cells bear functional skin-homing receptors. *J Immunol* 177:4488-4494.
22. Hale, G., Cobbold, S.P., Waldmann, H., Easter, G., Matejtschuk, P., and Coombs, R.R. 1987. Isolation of low-frequency class-switch variants from rat hybrid myelomas. *J Immunol Methods* 103:59-67.
23. Wing, K., Onishi, Y., Prieto-Martin, P., Yamaguchi, T., Miyara, M., Fehervari, Z., Nomura, T., and Sakaguchi, S. 2008. CTLA-4 control over Foxp3+ regulatory T cell function. *Science* 322:271-275.
24. Reiss, Y., Proudfoot, A.E., Power, C.A., Campbell, J.J., and Butcher, E.C. 2001. CC chemokine receptor (CCR)4 and the CCR10 ligand cutaneous T cell-attracting chemokine (CTACK) in lymphocyte trafficking to inflamed skin. *J Exp Med* 194:1541-1547.
25. Randolph, G.J., Ochando, J., and Partida, S.N.S. 2007. Migration of

Dendritic Cell Subsets and their Precursors. *Annu Rev Immunol.*
26. Yurchenko, E., Tritt, M., Hay, V., Shevach, E.M., Belkaid, Y., and Piccirillo, C.A. 2006. CCR5-dependent homing of naturally occurring CD4+ regulatory T cells to sites of Leishmania major infection favors pathogen persistence. *J Exp Med* 203:2451-2460.
27. Baekkevold, E.S., Wurbel, M.A., Kivisakk, P., Wain, C.M., Power, C.A., Haraldsen, G., and Campbell, J.J. 2005. A role for CCR4 in development of mature circulating cutaneous T helper memory cell populations. *J Exp Med* 201:1045-1051.
28. Huehn, J., Siegmund, K., Lehmann, J.C., Siewert, C., Haubold, U., Feuerer, M., Debes, G.F., Lauber, J., Frey, O., Przybylski, G.K., et al. 2004. Developmental stage, phenotype, and migration distinguish naive- and effector/memory-like CD4+ regulatory T cells. *J Exp Med* 199:303-313.
29. Banz, A., Peixoto, A., Pontoux, C., Cordier, C., Rocha, B., and Papiernik, M. 2003. A unique subpopulation of CD4+ regulatory T cells controls wasting disease, IL-10 secretion and T cell homeostasis. *Eur J Immunol* 33:2419-2428.
30. Zhang, N., Schroppel, B., Lal, G., Jakubzick, C., Mao, X., Chen, D., Yin, N., Jessberger, R., Ochando, J.C., Ding, Y., et al. 2009. Regulatory T cells sequentially migrate from inflamed tissues to draining lymph nodes to suppress the alloimmune response. *Immunity* 30:458-469.
31. Ring, S., Oliver, S.J., Cronstein, B.N., Enk, A.H., and Mahnke, K. 2009. CD4+CD25+ regulatory T cells suppress contact hypersensitivity reactions through a CD39, adenosine-dependent mechanism. *J Allergy Clin Immunol* 123:1287-1296 e1282.
32. Siegmund, K., Feuerer, M., Siewert, C., Ghani, S., Haubold, U., Dankof, A., Krenn, V., Schon, M.P., Scheffold, A., Lowe, J.B., et al. 2005. Migration matters: regulatory T-cell compartmentalization determines suppressive activity in vivo. *Blood* 106:3097-3104.
33. Miyara, M., Yoshioka, Y., Kitoh, A., Shima, T., Wing, K., Niwa, A., Parizot, C., Taflin, C., Heike, T., Valeyre, D., et al. 2009. Functional delineation and differentiation dynamics of human CD4+ T cells expressing the FoxP3 transcription factor. *Immunity* 30:899-911.
34. Kabashima, K., Arima, Y., and Miyachi, Y. 2003. Contact dermatitis from lacquer in a 'Go' player. *Contact Dermatitis* 49:306-307.
35. Kabashima, K., Murata, T., Tanaka, H., Matsuoka, T., Sakata, D., Yoshida, N., Katagiri, K., Kinashi, T., Tanaka, T., Miyasaka, M., et al. 2003. Thromboxane A2 modulates interaction of dendritic cells and T cells and regulates acquired immunity. *Nat Immunol* 4:694-701.

FIGURE LEGENDS

Figure 1. Cell migration from the skin to the DLN in the steady state.

(A) Kaede-Tg mice were photoconverted on the clipped abdominal skin as described in Methods and observed with a fluorescence stereoscopic microscope. Non-photoconverted clipped skin is shown as a control (middle). (Note: non-clipped area remains black since light cannot reach.) (B) Skin and draining axillary LN cells resected immediately after violet light exposure of the abdominal skin, and resected skin cells not exposed to violet light were subjected to flow cytometric analysis to evaluate the photoconversion. (C, D) Twenty-four h after photoconversion of the abdominal skin, cells from the draining axillary and other non-draining cervical and popliteal peripheral LNs were stained with CD11c and CD4 mAbs (C) and CD4 and CD44 mAbs (D), and subjected to flow cytometry. These data are representative of at least 5 experiments. Numbers within plots or histograms (B-D) indicate percentage of cells in the respective areas.

Figure 2. Migration of Tregs from the skin to DLNs.

(A-E) The DLN cells of Kaede/Foxp3$^{hCD2/hCD52}$ mice photoconverted on the abdomen 24 h prior were stained with CD4, CD25, and hCD2 mAbs. Shown here are the flow cytometric plots for hCD2/Foxp3 and CD25 staining among $CD4^+$ cells (A), and Kaede-red and Kaede-green expression on $hCD2^+CD4^+$ cells among skin-DLN cells (B). (C) The DLNs and non-DLNs from the mice 24 h after photoconversion were stained with CD4, hCD2, and CD44 mAbs, and subjected to flow cytometry. (D) hCD2/Foxp3 expression in total (Kaede-red plus Kaede-green), Kaede-red, and Kaede-green CD4 cells were compared by flow cytometry. (E) The numbers of $CD44^{mid}$ naïve (M), $CD44^{high}$ memory (H) and naïve plus memory (H/M) phenotypes of $hCD2^-CD4^+$ non-Tregs (-), $hCD2^+CD4^+$ Tregs (+), and total ($hCD2^-$ and $hCD2^+$; +/-) $CD4^+$ T cells in total $CD4^+$ (Kaede-red plus Kaede-green) cells and Kaede-red

cells in the DLNs were counted. Data are presented as means + SD and a representative of three independent experiments. The Student's *t* test was performed between the indicated groups and * indicates P <0.05. Numbers within plots or histograms indicate percentage of cells in the respective areas (A-D).

Figure 3. Cell migration from the skin to DLN during a cutaneous immune response.

(A) The scheme of the experimental protocol: The dorsal skin of Kaede/Foxp3$^{hCD2/hCD52}$ was sensitized, and 5 days thereafter the abdominal skin was challenged. Two days after challenge, the painted areas were photoconverted, and 24 h after photoconversion, cells from the skin-draining LNs were analyzed by flow cytometry. (B, C) The frequency of Kaede-red and Kaede-green cells among $CD4^+$ cells, and the frequencies of hCD2/Foxp3+ cells in total, Kaede-green, and Kaede-red cells among $CD4^+$ cells were analyzed. Numbers within plots or histograms indicate percentage of cells in the respective areas. (D) The numbers of $CD44^{mid}$ naïve (M), $CD44^{high}$ memory (H) and naïve plus memory (H/M) phenotypes of $hCD2^-CD4^+$ non-Tregs (-), $hCD2^+CD4^+$ Tregs (+), and total ($hCD2^-$ and $hCD2^+$; +/-) $CD4^+$ T cells among total $CD4^+$ cells and Kaede-red cells in the DLNs were counted. (E) The number of Tregs and non-Tregs in the skin: The mice were painted with DNFB or vehicle on the abdomen, followed by DNFB or vehicle application on the ears. The number of $CD4^+$ Tregs and $CD4^+$ non-Tregs, and the % ratio of Tregs among $CD4^+$ T cells in the ears were measured. (F) Transwell assay: The number of $hCD2^+CD4^+$ cells and $CD11c^+$ cells of skin cell suspensions from Foxp3$^{hCD2/hCD52}$ mice that migrated to lower chamber was analyzed. Data are presented as means + SD (D, E, and F) and are representative of three independent experiments. The Student's *t* test was performed between the indicated groups and * indicates P <0.05 (D, E, and F).

Figure 4. Enhanced ear swelling response by Treg depletion, and immunosuppressive activity of Treg subsets on T cell proliferation *in vitro*.

(A) The number of Tregs in the LNs after administration of Campath-1G Ab. (B) CHS: The Kaede/Foxp3$^{hCD2/hCD52}$ mice were sensitized, and injected with vehicle or Campath-1G Ab before challenge (n=8 for each group). (C-F) Immunosuppressive activity of Tregs: Kaede-red and Kaede-green Tregs were sorted from the Kaede/Foxp3$^{hCD2/hCD52}$ mice sensitized, challenged, and photoconverted. (C) Skin-DLN cells of mice sensitized with DNFB were stimulated with DNBS in the presence or absence of Kaede-red Tregs or Kaede-green Tregs *in vitro* (n=3). (D) Suppressive effect of Tregs *in vitro*: Kaede-red and Kaede-green Tregs were prepared as above, and added to T cells stimulated with plate-bound anti-CD3 Ab. (E) Antigen specificity of Treg functions: LN cells from DNFB-sensitized or TNCB-sensitized mice were stimulated with DNBS or TNBS *in vitro*. Kaede-red and Kaede-green Tregs were added, and percentage inhibition of cell proliferation was evaluated as (cell proliferation with DNBS or TNBS)-(cell proliferation with DNBS or TNBS in the presence of Tregs)/(cell proliferation with DNBS or TNBS)-(cell proliferation with vehicle) x 100. (F) Quantitative RT-PCR analysis on mRNA for *Il10* (IL-10) and *Tgfb1* (TGF-β), and *Ctla4* (CTLA-4) of Kaede-red Tregs and Kaede-green Tregs: The expression of each gene was normalized by the expression of *Gapdh*, and those in Kaede-green non-Tregs were normalized to one (n=3). Data are representative of three independent experiments and presented as means + SD (A-F). * indicates $P<0.05$ between the indicated groups (Student's *t* test, A, B, E, and F; one-way ANOVA followed by Dunnett multiple comparison test, C and D).

Figure 5. Immunosuppressive effect of Kaede-red Tregs in the skin.

(A) Suppression of CHS response by Kaede-red Tregs. Kaede-red or Kaede-green Tregs (4 x 10^3 cells/ear) of Kaede/Foxp3$^{hCD2/hCD52}$ mice sensitized, challenged, and photoconverted as in Figure 3A were injected into ear skin of mice sensitized with DNFB 5 days prior. Immediately after injection, the mice were challenged, and the ear thickness change was measured at 48, 72, and 96 h after challenge. (B-D) The mice were sensitized, challenged, and photoconverted as in Figure 3A. Twenty-four hours after photoconversion, 20 μl of 0.3% DNFB (challenge; +) or vehicle (challenge; -) (B), or 20 μl of 0.3% DNFB or 20 μl of 1% TNCB (C) was painted onto the ear. Twenty-four h later, the ear skin and blood (D) were collected and dissociated for flow cytometry. The number of Kaede-red Tregs in the skin and the frequency of Kaede-red Tregs in $CD4^+$ T cell subset of the blood were evaluated (n=3, each group). Data are presented as means + SD and representative of three independent experiments (A-C). The Student's *t* test was performed between the indicated groups and * indicates $P<0.05$. Numbers within plots indicate percentage of cells in the respective areas (D).

Figure 6. Surface molecule expressions on Kaede-red and Kaede-green cells.

(A) Chemokine receptor expression: Skin DLN cells were prepared from the mice sensitized, challenged and photoconverted as in Figure 3A. These LN cells were stained with isotype-matched control, CCR4, CCR5, and CCR7 mAbs, and the expression levels of Kaede-red and Kaede-green Tregs were evaluated by flow cytometry. (B) Transwell assay: The DLN cells were transferred to the upper chamber of the transwell, and CCL17 or CCL21 was added to the lower chamber. The cells were incubated for 3 h, and the numbers of Kaede-red and Kaede-green cells that migrated to lower chamber were analyzed by flow cytometry. Data are presented as means + SD and representative of two independent experiments. The Student's *t* test was performed between the indicated groups and * indicates $P<0.05$. (C) Surface

molecule expression: The LN cells were stained with isotype-matched control, CD62L, CD44, CD69, CD25, and CD103 mAbs, and the expression levels were evaluated by flow cytometry. These data are a representative of three independent experiments.

Figure 7. Kinetics and suppression activity of CD25^{high} Kaede-red migratory Tregs.

(A-C) Characterization of CD25^{high} subset: Kaede/Foxp3$^{hCD2/hCD52}$ mice were treated as in Figure 3A, and the expression levels of hCD2/Foxp3 and CD25 on CD4^{+}hCD2/Foxp3^{+} Tregs in total, Kaede-red and Kaede-green DLN cells and in non-DLN cells (A), the frequency of Kaede-red populations in each population (B), and the expression levels of surface markers on Kaede-red or Kaede-green Tregs in the DLNs (C) were analyzed. (D) Kinetics of T cell migration: Kaede/Foxp3$^{hCD2/hCD52}$ mice were sensitized and challenged as in Figure 3A, and photoconverted immediately (Day 0), 1 (Day 1), 2 (Day 2), or 3 (Day 3) days after challenge. The number of each subset migrating for 24 h after photoconversion and the frequency of Kaede-red cells among each subset were measured. (E) Foxp3$^{hCD2/hCD52}$ mice were sensitized with DNFB (S+), and challenged with DNFB (C+) or vehicle (C-). The skin suspensions were evaluated for the expression of hCD2/Foxp3 and CD25. (F) Skin-DLNs cells of sensitized-B6 mice were stimulated in the absence or presence of Kaede-red total hCD2^{+} Tregs (25$^{hi/int}$), CD25^{high} Tregs (25^{hi}) or CD25^{int} Tregs (25^{int}). (G) mRNAs for *Il10* (IL-10), *Tgfb1* (TGF-β) and *Ctla4* (CTLA-4) of Kaede-green CD25^{int} or CD25^{high} Tregs, Kaede-red CD25^{int} or CD25^{high} Tregs, or Kaede-green CD25^{int} Tregs in DLNs (D) or non-DLNs (N) were evaluated. The expression level in Kaede-green CD25^{int} Tregs was normalized to one. Data are presented as means + SD (n=3) (D, F, and G). *, $P<0.05$ between indicated groups. (F and G). Numbers within plots or histograms indicate percentage of cells (A, B, and E).

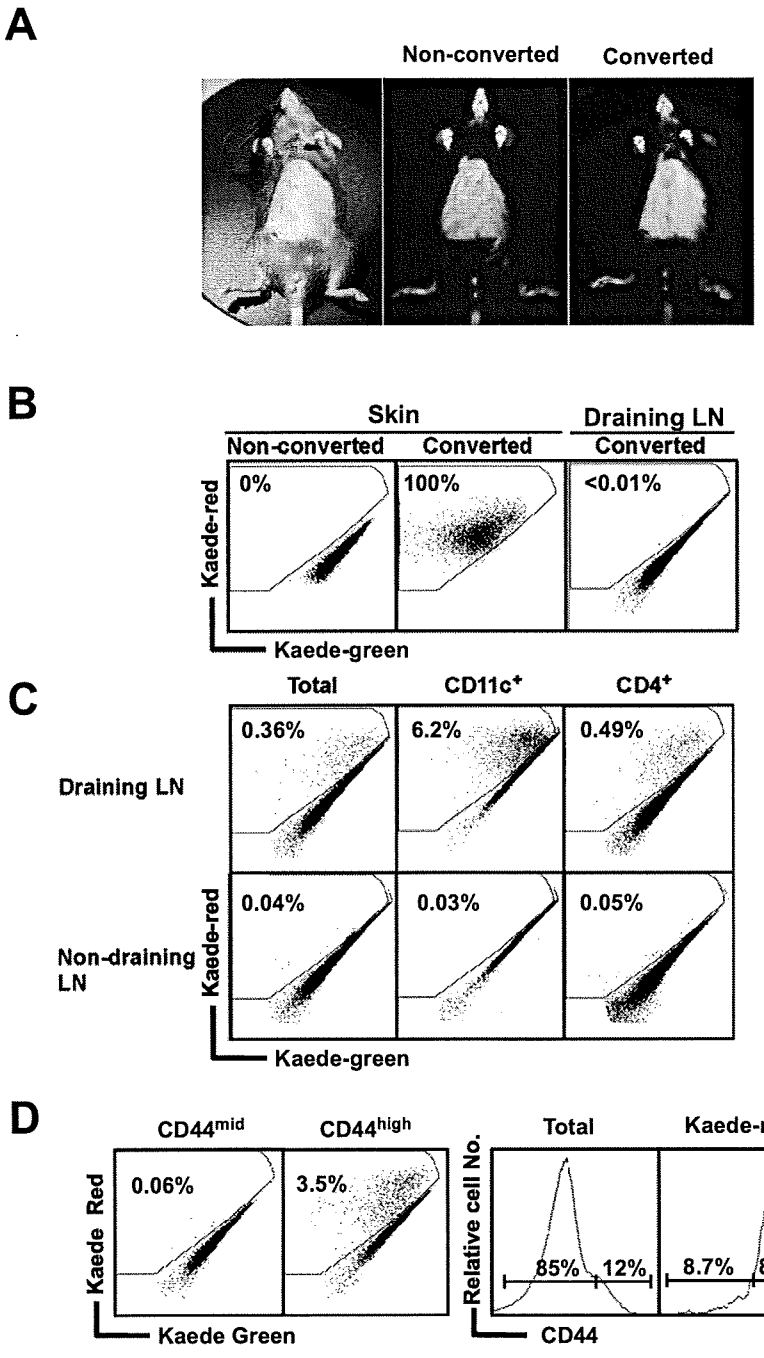
A
Non-converted
Converted
B
Skin
Draining LN
Non-converted
Converted
Converted
0%
100%
<0.01%
Kaede-red
Kaede-green
C
Total
CD11c+
CD4+
Draining LN
0.36%
6.2%
0.49%
Non-draining LN
0.04%
0.03%
0.05%
Kaede-red
Kaede-green
D
CD44mid
CD44high
0.06%
3.5%
Kaede Red
Kaede Green
Total
Kaede-red
Relative cell No.
85%
12%
8.7%
86%
CD44

Figure 1

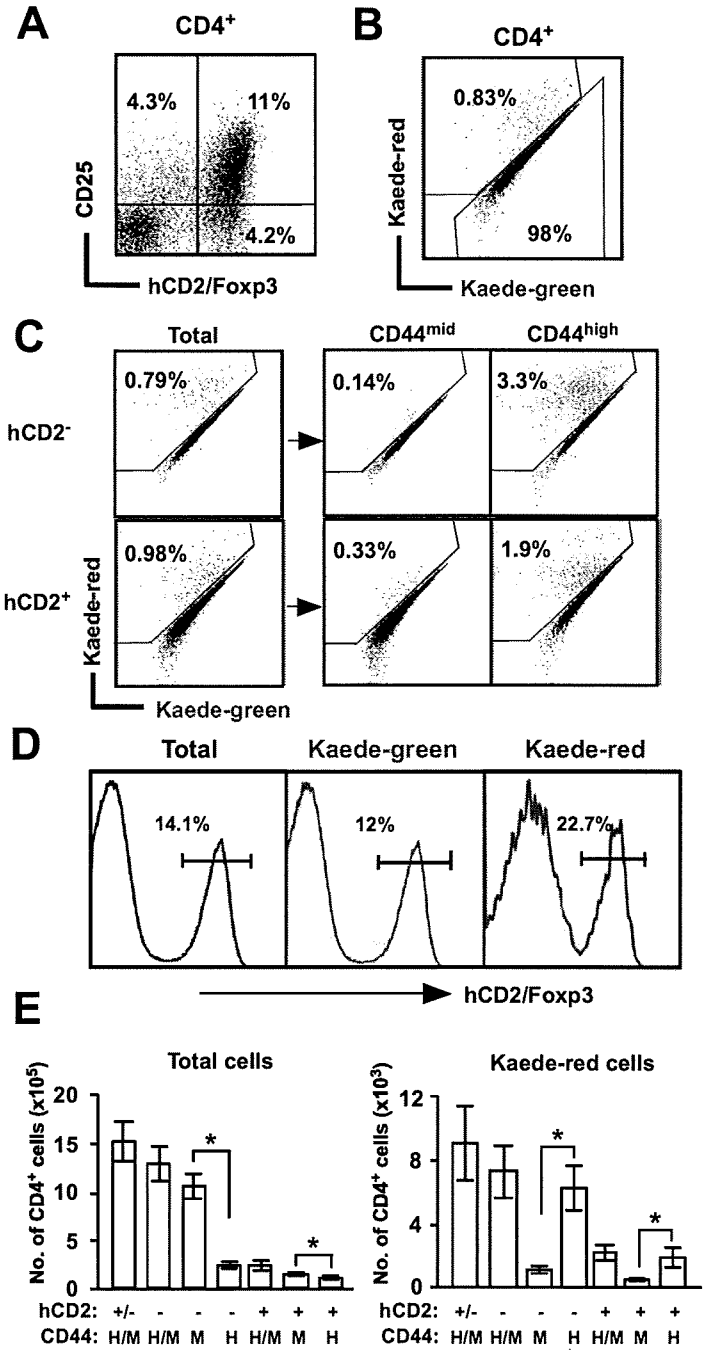
A
CD4+
4.3%
11%
4.2%
CD25
hCD2/Foxp3
B
CD4+
0.83%
98%
Kaede-red
Kaede-green
C
Total
CD44mid
CD44high
hCD2-
hCD2+
0.79%
0.14%
3.3%
0.98%
0.33%
1.9%
Kaede-red
Kaede-green
D
Total
Kaede-green
Kaede-red
14.1%
12%
22.7%
hCD2/Foxp3
E
Total cells
Kaede-red cells
No. of CD4+ cells (x10^5)
No. of CD4+ cells (x10^3)
hCD2: +/- - - - + + +
CD44: H/M H/M M H H/M M H

Figure 2

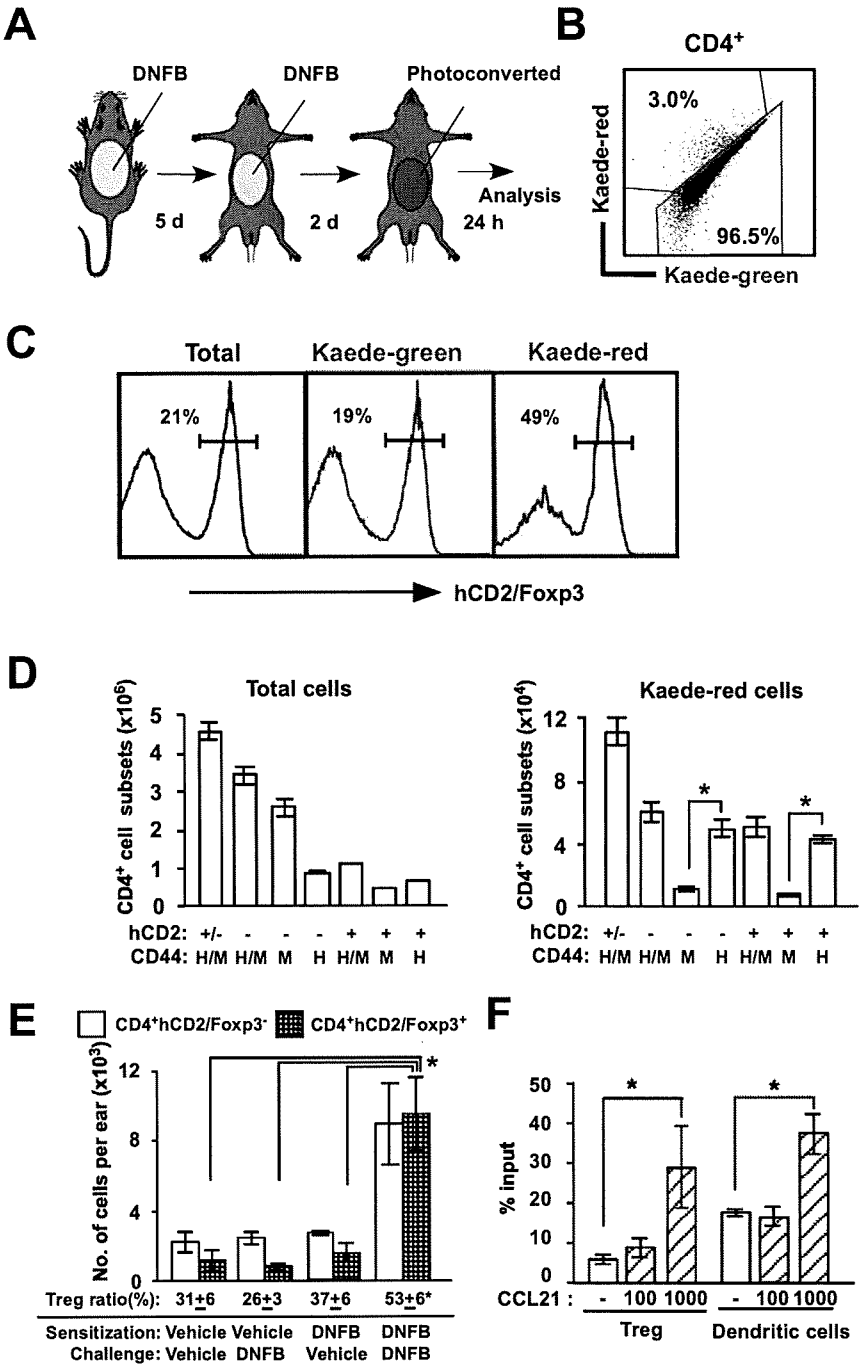
A
DNFB
DNFB
Photoconverted
5 d
2 d
Analysis
24 h
B
CD4+
3.0%
96.5%
Kaede-red
Kaede-green
C
Total
Kaede-green
Kaede-red
21%
19%
49%
hCD2/Foxp3
D
Total cells
Kaede-red cells
CD4+ cell subsets (x10^6)
CD4+ cell subsets (x10^4)
hCD2: +/- - - - + + +
CD44: H/M H/M M H H/M M H
E
CD4+hCD2/Foxp3- CD4+hCD2/Foxp3+
No. of cells per ear (x10^3)
Treg ratio(%): 31±6 26±3 37±6 53±6*
Sensitization: Vehicle Vehicle DNFB DNFB
Challenge: Vehicle DNFB Vehicle DNFB
F
% input
CCL21 : - 100 1000 - 100 1000
Treg
Dendritic cells

Figure 3

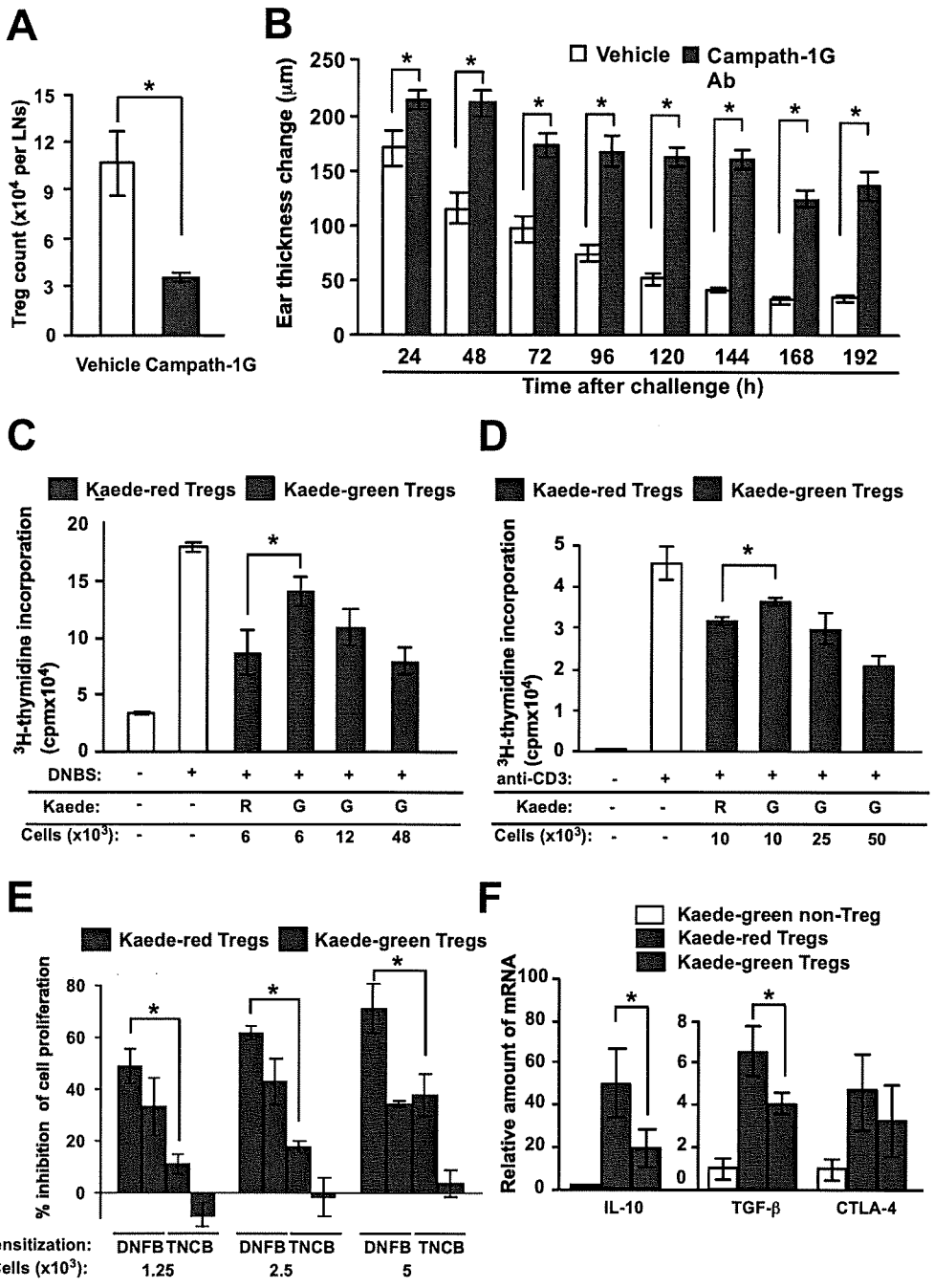
A
Treg count (x10⁴ per LNs)
Vehicle Campath-1G
B
Vehicle
Campath-1G Ab
Ear thickness change (μm)
Time after challenge (h)
C
Kaede-red Tregs
Kaede-green Tregs
³H-thymidine incorporation (cpmx10⁴)
DNBS:
Kaede:
Cells (x10³):
D
Kaede-red Tregs
Kaede-green Tregs
³H-thymidine incorporation (cpmx10⁴)
anti-CD3:
Kaede:
Cells (x10³):
E
Kaede-red Tregs
Kaede-green Tregs
% inhibition of cell proliferation
Sensitization:
Cells (x10³):
DNFB TNCB
1.25
2.5
5
F
Kaede-green non-Treg
Kaede-red Tregs
Kaede-green Tregs
Relative amount of mRNA
IL-10
TGF-β
CTLA-4

Figure 4

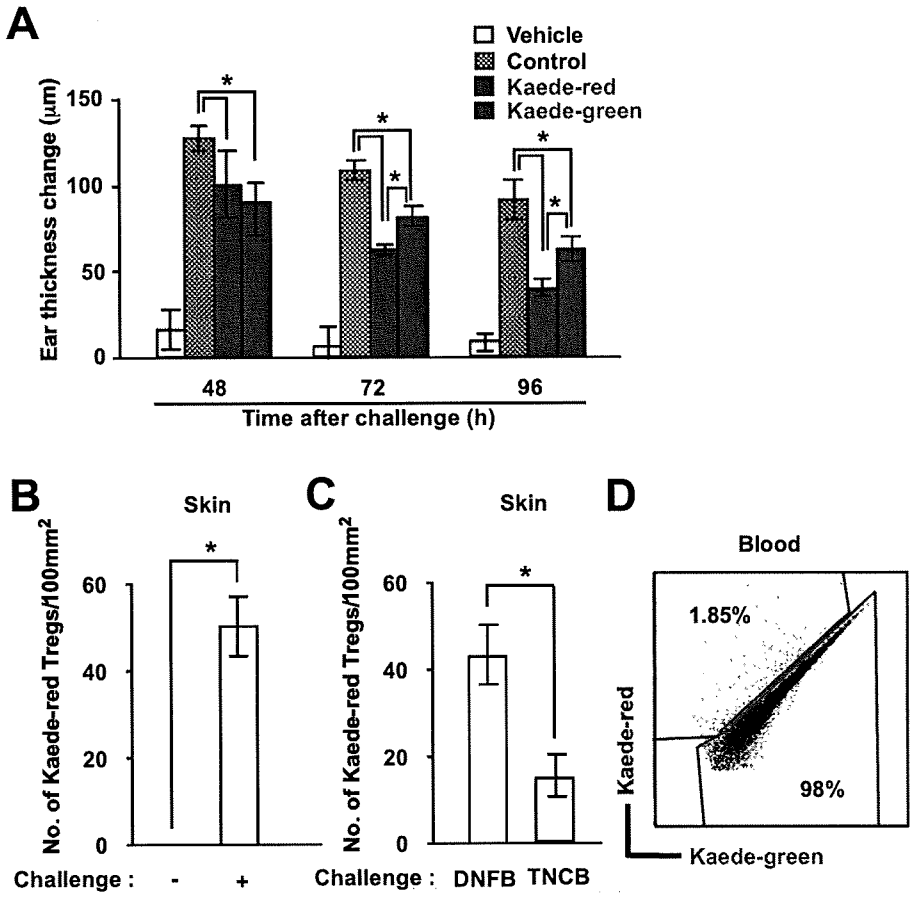
A
Vehicle
Control
Kaede-red
Kaede-green
Ear thickness change (μm)
150
100
50
0
48
72
96
Time after challenge (h)
B
Skin
No. of Kaede-red Tregs/100mm2
60
40
20
0
Challenge : - +
C
Skin
No. of Kaede-red Tregs/100mm2
60
40
20
0
Challenge : DNFB TNCB
D
Blood
1.85%
98%
Kaede-red
Kaede-green

Figure 5